Preprints of the 2012 20th Mediterranean Conference on Control & Automation (MED), Barcelona, Spain, July 3-6, 2012

Experimental inverted pendulum unfalsified control

Paulo Felício
Escola Superior de Tecnologia de Setúbal
Instituto Politécnico de Setúbal
Campus do IPS, Estefanilha
2910-761 Setúbal, Portugal
pfelicio@est.ips.pt

José Azinheira
Instituto Superior Técnico
Avenida Rovisco Pais, 1
1049-001 Lisboa, Portugal

Pedro Lourtie
Instituto Superior Técnico
Avenida Rovisco Pais, 1
1049-001 Lisboa, Portugal

***Abstract*— Unfalsified control is applied to an experimental inverted pendulum in the lab. A non-linear model for the system is developed. Using a set of six candidate controllers, of which two are destabilizing, a supervisory program is built. Experimental results show the best controllers are selected most of the time. When a destabilizing controller is put in the loop it is quickly removed and the performance does not degrade significantly. The application shows unfalsified control can be useful for control adaptation to process changes, even knowing it can some times select destabilizing controllers.**

I. Introduction

Switching supervisory control is an important option when one needs to control a system that can have its dynamics changed with time, due to faults or any other cause, [1]. One approach, that is appealing because it allows to deal with non-linear and ill-known systems is unfalsified control [2], [3], [4], in one of its forms. It allows on-line evaluation of candidate controllers in a supervisory switching control scheme, without putting them in the real loop. However, as mentioned in [5], [6], unfalsified control can put destabilizing controllers in the loop and that can sometimes lead to unacceptable performance. In spite of that, it is a useful method, as shown here.

In the present work, experimental system behavior is non-linear and it is assumed it can change with time. Supervisory switching control schemes that are based on system identification are not useful here because, although a good model is available, if the dynamics change, the identification of new model parameters is not easy, the lack of encoder resolution prevents rod-model identification. Even if that was not the case, the presence of unstable poles and zeros would make identification difficult.

II. Experimental system and non-linear model

Consider an inverted pendulum on a cart[1], shown in Fig. 1. The cart is driven by a dc motor and a belt. Control is done by a computer equipped with a data acquisition card receiving data from two encoders, coding cart position and pendulum angle, and sending a number $u(t) \in [-1,1]$ to an amplifier generating a voltage, $v_a(t)$, to drive the motor. System behavior is non-linear and although the model is not used in the supervisory control algorithms described here, it is useful for an understanding of the non-linearities involved and for numerical simulation experiments prior to lab experiments with the physical system.

Consider the loop in Fig. 3. Experiments revealed that modeling the amplifier and the motor is important if one wants to reproduce system behavior. Friction and measurements quantization are also important for that purpose.

Fig. 1. Experimental system in the lab.

A. Global non-linear model

1) Amplifier modeling : Amplifier gain is not linear. It was modeled as a function of input value as $g_a(u)$ in (1). This results in a static model, $v_a = g_a(u) \times u$, obtained from experimental input-output measurements. Parameter values for $g_a(u)$ are $a = 12.01$, $b = -7.388$, $c = 21.85$ and $d = -0.09029$.

$$g_a(u) = \begin{cases} 27.4 & \text{if} \quad u \in]-0.1, 0.1[\\ ae^{b|u|} + ce^{d|u|} & \text{if} \quad u \in [-1,-0.1] \cup [0.1,1] \end{cases} \tag{1}$$

2) Cart friction force estimate: Friction modelling can be complex. There are static and dynamic effects and hysteresis can occur. Some references on friction compensation by control can be found in [7] and [8]. About dry friction in particular see [9]. Several models were considered for the cart friction force description, including speed dependent forces and the Stribeck effect. The best solution for the present case was to use a constant magnitude friction force $\bar{f}_a = 2.56N$. To include cart friction force effects in the model, an equivalent torque, acting against motor axis movement is considered.

3) Encoders quantization: Both measurements, for rod angle and cart position, are done using rotational incremental encoders. Each encoder can distinguish 2048 different positions. For the rod angular position, $\theta(t)$, the quantization

[1]The system is built by Feedback Instruments Ltd, Park Road, Crowborough, E. Sussex, TN6 2QR, UK.

978-1-4673-2529-5/12/$31.00 ©2012 IEEE

is q_θ in (2). For cart position measurement, $x_c(t)$, the quantization is q_{x_c} in (3).

$$q_\theta = \frac{2\pi}{2048} = 3.068 \times 10^{-3}\ rad \tag{2}$$

$$q_{x_c} = \frac{q_\theta}{K_c} = 0.079 \times 10^{-3}\ m \tag{3}$$

Although the quantization intervals for θ and x_c can seem rather small, they are relevant for the closed loop system behaviour. The way in which values for the derivatives $\dot{\theta}$ and $\dot{x_c}$ are obtained, by computation from the discrete measurements, also contribute to quantization relevance.

4) Inverted pendulum model: Considering only the cart and the rod, the inverted pendulum model can be derived using Lagrangeans. The resulting equations are included in the non-linear model from (4) to (12). Parameters are $m = 0.120kg$ for rod mass, $l = 0.178m$ for rod center of mass distance to the pendulum pivot, $I_{cmh} = 0.001815kg \cdot m^2$ for rod inertia around its center of mass, $M = 1.185kg$ for cart mass, and $f_p = 0.000101N \cdot (rad \cdot s^{-1})^{-1}$ is a friction coefficient for the rotational movement of the rod. All parameters were measured or experimentally determined, for f_p see for example [10], p.376.

5) Motor, cart and rod model: The motor used to move the pendulum is an armature controlled dc motor, with constant field. The motor is manufactured by Crouzet with reference 82850002. Although a complex device, it can be modeled by a well known simple set of equations, see for example [11]. Equation (4) describes the motor electrical behavior. $i_a = i_a(t)$ stands for motor armature current and $\theta_m = \theta_m(t)$ for its angular displacement. Parameters are $R_a = 2.5\Omega$, $L_a = 0.0025H$ and $K_e = 0.0522V \cdot (rad \cdot s^{-1})^{-1}$.

$$\frac{di_a}{dt} = -\frac{K_e}{L_a}\dot{\theta}_m - \frac{R_a}{L_a}i_a + \frac{1}{L_a}v_a \tag{4}$$

Equations (5) and (6) describe the system mechanical behavior and include motor, cart and rod, which are coupled. Motor angular movement and cart linear movement are related by $x_c(t) = (K_c)^{-1}\theta_m(t)$ with $K_c = 38.6492m^{-1}$. Force on the cart is related to motor torque by $f(t) = K_u T(t)$, where the value for $K_u = K_c$. There is also a constant, $K_t = 0.0522N \cdot m \cdot A^{-1}$, relating motor torque to armature current, as $T(t) = K_t i_a(t)$. Fiction coefficient in motor shaft is $b = 0.151 \times 10^{-3} N \cdot (m \cdot s^{-1})^{-1}$ and the inertia moment for the motor and the belt pulleys is $J_{m2} = 4.4 \times 10^{-5} kg \cdot m^2$.

$$\left(J_{m2} + \frac{M+m}{K_u K_c}\right)\ddot{\theta}_m = K_t i_a - b\dot{\theta}_m + \frac{ml}{K_u}(\sin\theta)\dot{\theta}^2 + \\ - \frac{ml}{K_u}(\cos\theta)\ddot{\theta} - \frac{\bar{f}_a}{K_u}\frac{\dot{\theta}_m}{|\dot{\theta}_m|} \quad , \quad \dot{\theta}_m \neq 0 \tag{5}$$

$$\ddot{\theta} = \frac{lmg}{I_{cmh} + ml^2}(sen\theta) - \frac{lm}{K_c(I_{cmh} + ml^2)}(\cos\theta)\ddot{\theta}_m + \\ - \frac{f_p}{I_{cmh} + ml^2}\dot{\theta} \tag{6}$$

Differential equations (4), (5) and (6) constitute a non-linear model for the system, including motor, cart and rod. They are valid for $\dot{\theta}_m \neq 0$. When $\dot{\theta}_m = 0$, there is static friction corresponding to the motor dead-zone, and equation (5) should be replaced. What changes is friction force, or equivalent torque. Signal $\ddot{\theta}_m$ is then computed as:
If

$$\left| K_t i_a - b\dot{\theta}_m + \frac{lm}{K_u}(\sin\theta)\dot{\theta}^2 - c_3(cos\theta)(\sin\theta) \right. \\ \left. + c_4(\cos\theta)\dot{\theta} \right| < \frac{\bar{f}_a}{K_u} \tag{7}$$

then $\ddot{\theta}_m = 0$.
Else, if

$$K_t i_a - b\dot{\theta}_m + \frac{lm}{K_u}(\sin\theta)\dot{\theta}^2 - c_3(cos\theta)(\sin\theta) + c_4(\cos\theta)\dot{\theta} < 0 \tag{8}$$

$$\text{then} \quad \ddot{\theta}_m = \frac{1}{c_1 + c_2(\cos\theta)^2}\left[K_t i_a - b\dot{\theta}_m + \frac{lm}{K_u}(\sin\theta)\dot{\theta}^2 + \right. \\ \left. - c_3(cos\theta)(\sin\theta) + c_4(\cos\theta)\dot{\theta} + \frac{\bar{f}_a}{K_u}\right] \tag{9}$$

$$\text{else} \quad \ddot{\theta}_m = \frac{1}{c_1 + c_2(\cos\theta)^2}\left[K_t i_a - b\dot{\theta}_m + \frac{lm}{K_u}(\sin\theta)\dot{\theta}^2 + \right. \\ \left. - c_3(cos\theta)(\sin\theta) + c_4(\cos\theta)\dot{\theta} - \frac{\bar{f}_a}{K_u}\right] \tag{10}$$

In (7) to (10) the following constants are used.

$$c_1 = J_{m2} + \frac{M+m}{K_u K_c} \quad , \quad c_2 = \frac{(ml)^2}{K_u K_c (I_{cmh} + l^2 m)} \tag{11}$$

$$c_3 = \frac{(ml)^2}{K_u(I_{cmh} + ml^2)} \quad , \quad c_4 = \frac{ml f_p}{K_u(I_{cmh} + ml^2)} \tag{12}$$

Comparing lab experimental results with numerical simulation results shows this model is an adequate description for the experimental system behaviour. Fig. 2 shows simulation and experimental results for a cart reference position as described in (13).

$$\begin{cases} r_x(t) = 0 \quad \text{se} \quad t < 2 \ \vee t \ \geq 22.5 \\ r_x(t) = 0.2 \quad \text{se} \quad t \in [2,5] \\ r_x(t) = \frac{0.3}{25}(t-10)^2 - 0.1 \quad \text{se} \quad t \in [5,15] \\ r_x(t) = \frac{0.2}{5}t - 0.8 \quad \text{se} \quad t \in [15,22.5] \end{cases} \tag{13}$$

III. Supervisor

The feedback structure for the system is as shown in Fig. 3. Control in the loop is determined by a supervisory switching control algorithm that periodically selects the best controller, from a predefined candidate controllers set, based in measured data and in fictitious reference signals, [2], computed from it.

Experiments are done to test if this kind of supervisor can be successfully used in switching control, capable of appropriate reaction to system changes. That is done placing a bad controller in the loop, from time to time, instead of changing system dynamics, simply because it is an easier procedure. Those experiments are conceptually equivalent to a change in the process, resulting in bad performance or even unstable behavior, requiring supervision to replace the controller in the loop.

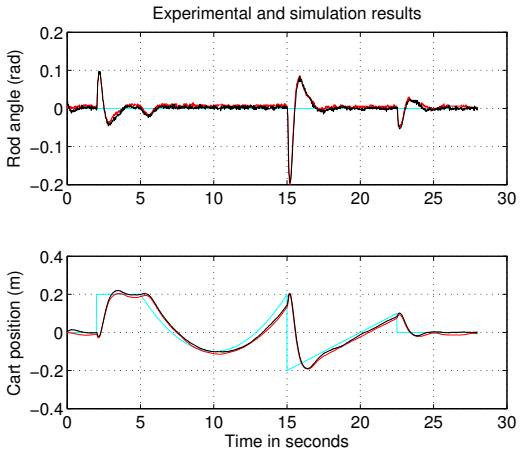

Fig. 2. Experimental results in red and simulation results in black. The cyan line shows the reference signal. $K11$ is in the loop.

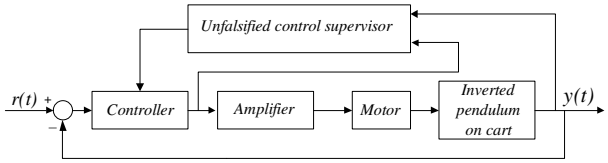

Fig. 3. Feedback system components with supervision.

A. Candidate controller set

Six state feedback controllers are considered, their gains described in (14) to (19). Although the system has more complexity, only four states are fed back, corresponding to those of a linearized model for an inverted pendulum on cart. The fed back states are $\alpha = \begin{bmatrix} \theta & \dot{\theta} & x_c & \dot{x}_c \end{bmatrix}^T$, for rod angular position and velocity and for cart position and velocity.

$$K11 = \begin{bmatrix} -16.12 & -2.62 & -8.41 & -5.40 \end{bmatrix} \quad (14)$$

$$K12 = \begin{bmatrix} -17.89 & -4.93 & -7.11 & -5.40 \end{bmatrix} \quad (15)$$

$$K13 = \begin{bmatrix} -13.44 & -2.18 & -7.00 & -4.50 \end{bmatrix} \quad (16)$$

$$K14 = \begin{bmatrix} -24.00 & -8.00 & -12.00 & -6.00 \end{bmatrix} \quad (17)$$

$$K15 = \begin{bmatrix} -20.00 & -5.00 & -6.00 & -6.00 \end{bmatrix} \quad (18)$$

$$K16 = \begin{bmatrix} -3.00 & -4.00 & -5.00 & -6.00 \end{bmatrix} \quad (19)$$

This controllers were first designed as optimal linear quadratic regulators for a linearized model. Due to system nonlinearities the original controllers were not appropriate and were manually adjusted, based on experiments with the non-linear model and the physical system.

For an idea of each controller's performance, Figs. 4 to 6 show the experimental time responses for the various controllers, for a step cart position reference of amplitude $0.2m$ occurring at $t = 2s$.

The set has two good performance controllers, K11 and K13, two inferior performance controllers K12 and K15, and two non stabilizing controllers, K14 e K16.

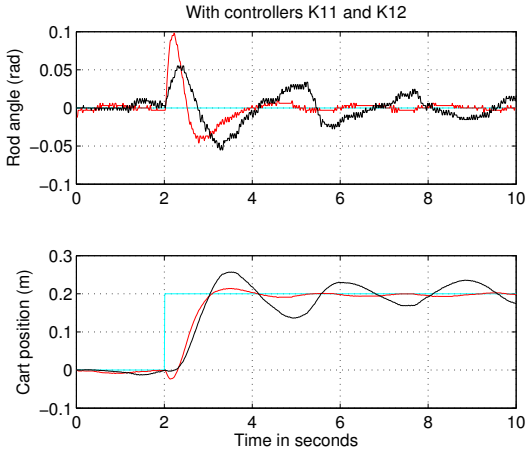

Fig. 4. Experimental performance of controllers K11, in red, and K12, in black. The cyan lines represent cart position and rod angle references.

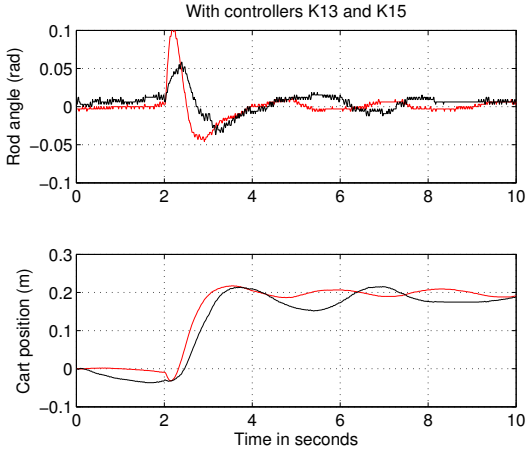

Fig. 5. Experimental performance of controller K13, in red, and K15, in black.

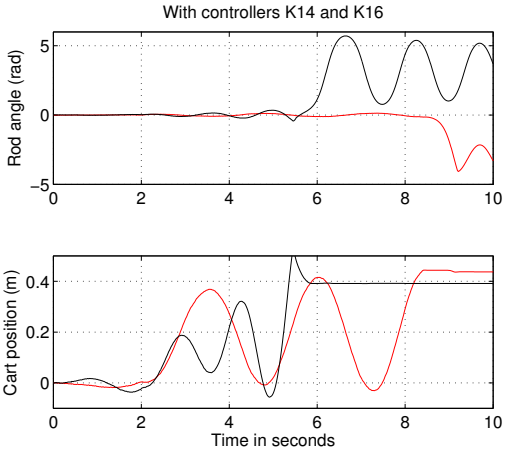

Fig. 6. Experimental performance of destabilizing controllers, K14, in red, and K16, in black.

B. Controller inversion and fictitious reference

Controllers are placed in the direct path in the loop, as shown in Fig. 3. State vector $\alpha = \begin{bmatrix} \theta & \dot{\theta} & x_c & \dot{x}_c \end{bmatrix}^T$, is fed back. In practice only angle θ and cart position, x_c, are measured, their derivatives being computed from them, discretely, according to (20). $T_s = 0.01s$ is the sampling period used for the measurements, the same period is used for control.

$$\dot{\theta}(t) = \frac{\theta(t) - \theta(t - T_s)}{T_s} \quad , \quad \dot{x_c}(t) = \frac{x_c(t) - x_c(t - T_s)}{T_s} \tag{20}$$

A state reference signal $r(t) = \begin{bmatrix} 0 & 0 & r_x(t) & 0 \end{bmatrix}^T$ is used and for a controller $K = \begin{bmatrix} k_1 & k_2 & k_3 & k_4 \end{bmatrix}$, the control signal, $u(t)$, is computed using (21).

$$u(t) = -k_1\theta(t) - k_2\dot{\theta}(t) + k_3(r_x(t) - x_c(t)) - k_4\dot{x_c}(t) \tag{21}$$

Solving (21) for $r_x(t)$ allows the computation of the reference signal that would have resulted in the recorded data, u and α, had controller K been in the loop during all the time of the experiment. That is the fictitious reference signal, $\tilde{r}_{Kx}(t)$, for controller K, in the unfalsified control sense, [2]. $\tilde{r}_{Kx}(t)$ is defined for $t \in [0, \tau]$, where τ is the present time instant. Note that one signal $\tilde{r}_{Kx}(t)$ can be computed for each controller K even if it is not in the loop.

$$\tilde{r}_{Kx}(t) = \frac{1}{k_3}\left[u(t) + k_1\theta(t) + k_2\dot{\theta}(t) + k_3x_c(t) + k_4\dot{x_c}(t)\right] \tag{22}$$

C. Controller evaluation

Controllers are evaluated using cost functional (23), which is a measure of the relative reference following error. Smaller cost v means a better controller. In $v(K,d,\tau)$, $d = (u,\alpha)$ is the data collected in $t \in [0,\tau]$ and K the controller whose cost is being computed.

$$v(K,d,\tau) = \frac{\|y(t) - \tilde{r}_K(t)\|_\tau^2}{\|\tilde{r}_K(t)\|_\tau^2 + \varsigma} \tag{23}$$

In (23) $y = \begin{bmatrix} \theta & x_c \end{bmatrix}^T$ and $\tilde{r}_K = \begin{bmatrix} 0 & \tilde{r}_{Kx} \end{bmatrix}^T$. The norm $\|\cdot\|_\tau$ is the usual Euclidean norm for signals, from 0 to τ, $\|\cdot\|_\tau = [\int_0^\tau < \cdot, \cdot > d\tau]^{\frac{1}{2}}$. A small value $\varsigma = 0.01$ is used to avoid divisions by zero and too high cost values at initial time instants. Those can occur for example if the reference is zero for some time.

To test controller's evaluation using (23), and the viability of switched control based on fictitious references, experiments were done closing the control loop with each of the first four candidate controllers, K11 to K14, and recording data $d = (u,\alpha)$. The same reference signal from section III-A, shown in cyan in Fig. 4 was used.

Figs. 7 to 9 show the result for controllers $K11$, $K12$ and $K14$. For controller $K13$ no plot is presented since it is practically equal to the one in Fig. 7.

Observing the plots for $v(K,d,\tau)$, it is expectable that controller evaluation by $v(K,d,\tau)$, allows the selection of adequate controllers to the system. If initially a bad performance controller is placed in the loop, $K12$ or $K14$, it should be quickly replaced by better performance $K11$ or $K13$. Even if a destabilizing controller is put in the loop it should be timely replaced by another, stabilizing and good performance controller. Here "timely" means before rod angle θ becomes too big.

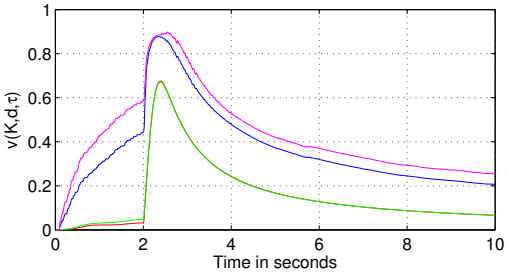

Fig. 7. Costs $v(K,d,\tau)$ with controller $K11$ in the loop. Red for $K11$ cost, blue for $K12$, green for $K13$ and magenta for $K14$.

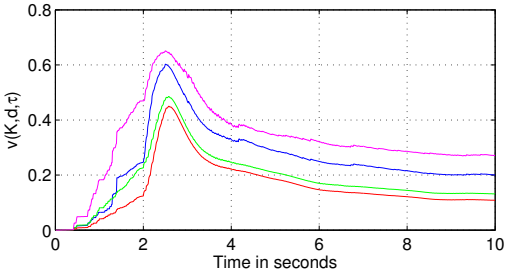

Fig. 8. Costs $v(K,d,\tau)$ with controller $K12$ in the loop. Red for $K11$ cost, blue for $K12$, green for $K13$ and magenta for $K14$.

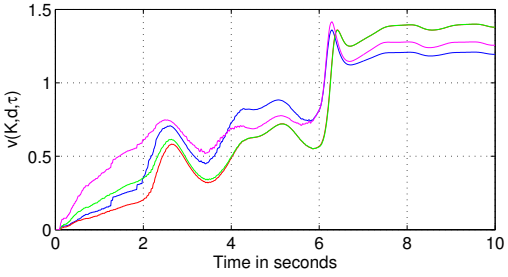

Fig. 9. Costs $v(K,d,\tau)$ with controller $K14$ in the loop. Red for $K11$ cost, blue for $K12$, green for $K13$ and magenta for $K14$.

Note the cost functional in (23) may not have properties such as monotonicity and cost detectability, usually required in unfalsified control theory to guarantee closed loop stability of the switched control system, see [12]. However the authors believe this is not relevant since known stability properties do not apply to the present case, because the system is not recoverable if, roughly, $\theta \notin [-0.4, 0.4]$ or $x_c \notin [-0.4, 0.4]$. Out of this bounds the system can not continue to work.

D. Supervisor implementation

Programs were written to implement control and supervision. The supervisory algorithm, that determines which controller

should be put in the loop, is programmed in Matlab and has a graphical interface, programmed using Simulink, that is shown in Fig. 10. The controllers, placed by the supervisor in the loop, are programmed in C as a DLL[2]. The DLL works as a real time kernel and computes the control signal at each sampling period of 0.01s.

Two supervisory algorithms, using cost function $v(K,d,\tau)$ in (23), were programmed. The first one uses data from the beginning of operation, the controllers being evaluated, using all data, at each 100 new data points. At each second the supervisor selects the least cost controller and commands the real time kernel to use it in computing the actuation signal. A dwell-time algorithm is used. No hysteresis is used because the 1 second *dwell time* is enough to avoid *dithering* and instability.

The second algorithm works in the same way, except that only data from the most recent second is used. That is, at each second the cost associated to each controller is computed using the 100 data points just collected. The lower cost controller is placed in the loop.

The graphical interface shown in Fig. 10 allows the operator to put the system to work, to command manually the controller in the loop, to move the cart to the left or the right and to give order for one or the other supervisory algorithm to become active in determining the controller in the loop.

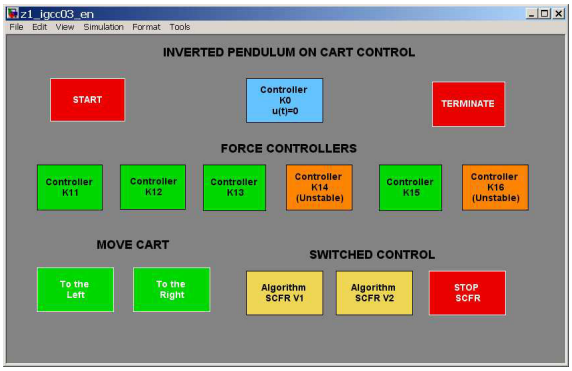

Fig. 10. Supervisor graphical interface.

IV. Experimental results

Both algorithms just described were applied using cost function $v(K,d,\tau)$ in (23), with the set of six controllers in (14) to (19). The result is the selection of controller $K11$ most of the time. Even if a destabilizing controller is put in the loop, it is quickly replaced by a good performance controller. This is true for both algorithms referred above.

First supervisory algorithm: Fig. 11 shows, in the lower plot, the cost associated to each controller. The upper plot in that figure presents the number of the controller in the loop. The controller initially in the loop, selected by us is controller $K12$. That controller is quickly removed from the loop by the automatic supervisory algorithm. All the selections of controllers different from $K11$, that can be observed in the plot are operators orders, to see how the algorithm reacts. The algorithm removes them from the loop immediately after collecting and using the first set of 100 data points, corresponding to 1s. The experiment was done with null reference, for both cart position and rod angle.

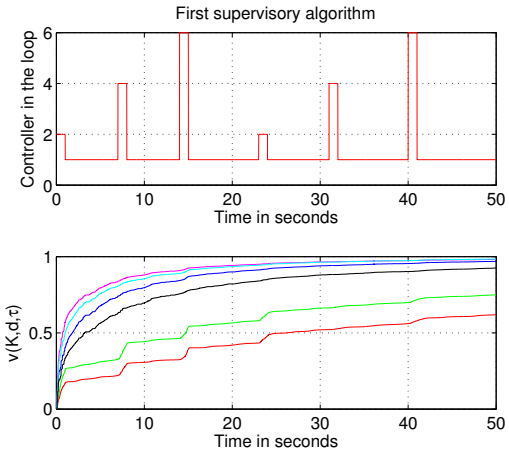

Fig. 11. Controller in loop in the upper plot; all controllers different from $K11$ were forced by the operator. Cost associated to each controller in the lower plot. Red: K11, green: K13, blue: K12, magenta: K14, cyan: K15, black: K16.

Second supervisory algorithm: With this algorithm the result is almost always the selection of one of the two best controllers, even if the operator places a destabilizing controller in the loop. Fig. 12 shows the result of a lab experiment with the inverted pendulum using the supervisory system. The thicker line, in black, shows the number for the controller in the loop. From time to time the operator places a different controller in the loop, even destabilizing controllers. Almost always, the algorithm does not need more than one second to select the best controller available and put it in the loop. The exception is the selection of controller $K16$ at $t = 32s$, when the algorithm takes 2 seconds to select the best controller. The plot in Fig. 12 shows the cost of each controller times 5, for better visualization. Fig. 13 presents a zoom for the first 12 seconds presented in Fig. 12. Fig. 14 shows the output signals for the same experiment.

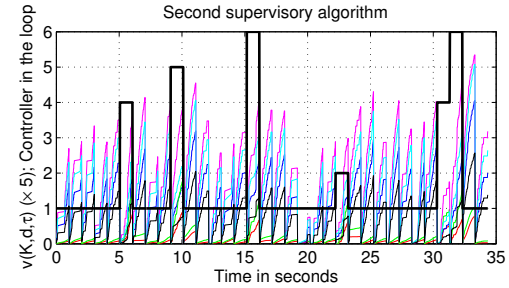

Fig. 12. Controller in the loop, in black. The colored lines represent cost associated to each controller, multiplied by 5; red: K11, green: K13, blue: K12, magenta: K14, cyan: K15, black: K16.

[2]DLL = Data Link Library

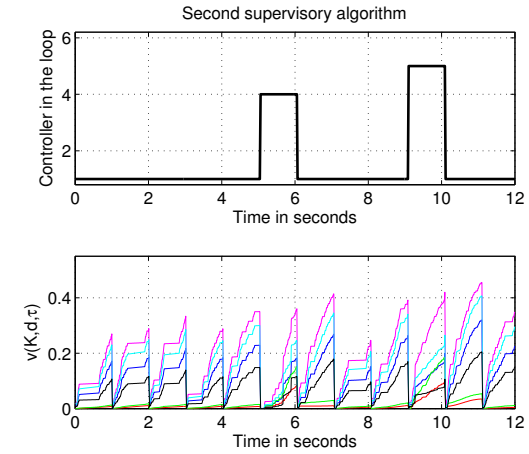

Fig. 13. Controller in the loop and cost associated to each controller. Red: K11, green: K13, blue: K12, magenta: K14, cyan: K15, black: K16.

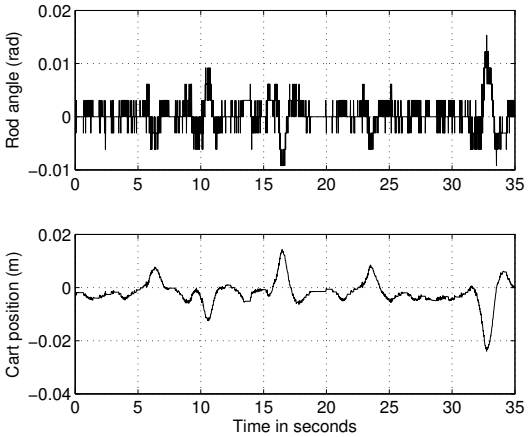

Fig. 14. Inverted pendulum experimental output values for θ and x_c for the same 35 seconds show in Fig. 12

Notes on the application: The application just described shows the supervisory algorithms based on fictitious reference signals select good performance controllers, although the ones of poor performance or destabilizing, are the majority in the set of candidate controllers. This for a real unstable process with non-linear behavior.

The second version of the supervisory algorithm is better as it can deal with time varying systems, because only data collected from the most recent second is used. This allows the switching to adequate controllers, if a change in the process demands such an action.

The fact the system has worked well does not constitute demonstration it can not perform badly. There is no proof the cost function always selects the appropriate controllers. In fact, when the operator placed $K15$ in the loop, near $t = 30s$, the supervisory algorithm selected controller $K16$. That controller stayed in the loop for 1 second, being replaced by $K11$. The performance degradation was not an important one.

Determination of the exact circumstances, when the good performance of this algorithms is guaranteed will be object of further study, in particular as to the kinds of controllers that give better results.

V. Conclusions

Unfalsified control can be successfully used for a supervisory switching adaptive control mechanism to react to controlled process changes. For the case of an experimental inverted pendulum, results were positive. Even if sometimes an unstable controller is selected, the supervisor acts quickly enough to remove such controller from the loop, before performance degradation is remarkable.

A process model can be used to design the candidate controllers set but it is not used by the supervisory system. The controllers are evaluated without need to put them in the loop, at least most times. When out of the loop evaluation fails, the bad performance controllers stayed in the loop for a short time.

This application shows the unfalsified control method may be successfully applied to non-linear unstable systems. That is true even if the system dynamics are not well known.

References

[1] J. P. Hespanha, "Tutorial on supervisory control," Lecture Notes for the workshop *Control using Logic and Switching* for the 40th Conf. on Decision and Contr., Orlando, Florida, Dec. 2001, available at http://www.ece.ucsb.edu/ hespanha/published.

[2] M. G. Safonov and T.-C. Tsao, "The unfalsified control concept and learning," *IEEE Transactions on Automatic Control*, vol. 42, no. 6, pp. 843–847, June 1997.

[3] M. G. Safonov, "Focusing on the knowable; controller invalidation and learning," in *Control Using Logic-Based Switching*, A.S.Morse, Ed. Springer Verlag, Berlin, 1996, pp. 224–233.

[4] H. Jin, M. W. Chang, M. Safonov, J. Zhu, and Z. Wang, "Unfalsified adaptive control: Inter-falsification and self-falsification," in *Proceedings of the 8th World Congress on Intelligent Control and Automation*, Taipei, Taiwan, June 21-25 2011.

[5] A. Dehghani, B. D. O. Andersen, and A. Lanzon, "Unfalsified adaptive control: A new controller implementation and some remarks," in *Proceedings of the European Control Conference*, Kos, Greece, June 2-5 2007, pp. 709–716.

[6] P. Felício and P. Lourtie, "A case study on multiple controller adaptive control," in *Proceedings of the 17th World Congress, The International Federation of Automatic Control*, Seul, Korea, July 6-11 2008, pp. 4875–4880.

[7] H. Olsson, K. J. Astrom, C. C. de Wit, M. Gafvert, and P. Lischinsky, "Friction models and friction compensation," *European Journal of Control*, vol. 4, no. 3, pp. 176–195, 1998.

[8] B. Armstrong and C. C. de Wit, *The Control Handbook*, 1996, ch. Friction modeling and compensation, pp. 1369–1382.

[9] J. Wojewoda, A. Stefanski, M. Wiercigroch, and T. Kapitaniak, "Hysteretic effects of dry friction: modelling and experimental studies," *Philosophical Transactions of the Royal Society*, no. 366, pp. 747–765, 2008.

[10] D. C. Giancoli, *Physics for Scientists and Engineers*, 3rd ed. Prentice Hall, 2000.

[11] G. F. Franklin, J. D. Powell, and A. Emami-Naeini, *Feedback Control of Dynamic Systems*, 3rd ed. Addison Wesley, 1994.

[12] M. Stefanovic and M. G. Safonov, *Safe Adaptive Control*, ser. Lecture Notes in Control and Information Sciences, No. 405. Springer Verlag. London, 2011.